



Research article

Synergistic effects of halloysite and carbon nanotubes (HNTs + CNTs) on the mechanical properties of epoxy nanocomposites

Mohd Shahneel Saharudin^{1,*}, Rasheed Atif², Syafawati Hasbi³, Muhammad Naguib Ahmad Nazri¹, Nur Ubaidah Saidin⁴ and Yusof Abdullah⁴

¹ Universiti Kuala Lumpur Malaysia Italy Design Institute (UniKL MIDI), 56100 Cheras, Kuala Lumpur, Malaysia

² Department of Mechanical and Construction Engineering, Northumbria University, Ellison Place, Newcastle upon Tyne NE1 8ST, United Kingdom

³ Department of Mechanical Engineering, National Defense University of Malaysia, 57000, Kuala Lumpur, Malaysia

⁴ Malaysian Nuclear Agency Bangi, 43000, Kajang, Selangor, Malaysia

* **Correspondence:** Email: mshahneel@unikl.edu.my; Tel: +60391795072; Fax: +60391795001.

Abstract: The synergistic effects of halloysite nanotubes (HNTs) and carbon nanotubes (CNTs) on the mechanical properties of epoxy nanocomposites were investigated. The addition of hybrid nanofillers (0.5 wt% HNTs–0.5 wt% CNTs) has significantly increased the storage modulus, flexural strength, tensile strength, fracture toughness (K_{IC}), critical strain energy release rate (G_{IC}), and microhardness of the nanocomposites. The tensile strength and Young's modulus increased up to approximately 45% and 49%, respectively. The flexural strength and modulus increased up to approximately 46% and 17%, respectively. K_{IC} , G_{IC} , and microhardness recorded improvements of up to approximately 125%, 134%, and 11%, respectively. The formation of a large number of microcracks (emanated radially) and the increase in fracture surface area (due to crack deflection) were the major toughening mechanisms in the hybrid nanocomposites. SEM images revealed that the hybrid nanofillers were uniformly dispersed in the epoxy matrix and the fracture surface was coarser than that of neat epoxy, suggesting a semi-ductile fracture. This study has shown that the synergistic effects of HNTs–CNTs hybrid nanocomposites at low content (0.5 wt% HNTs–0.5 wt% CNTs) have significantly enhanced the mechanical properties of epoxy nanocomposites.

Keywords: halloysite nanotubes (HNTs); carbon nanotubes (CNTs); epoxy; hybrid nanofillers; nanocomposites; mechanical properties

1. Introduction

Due to their low cost, reproducibility, and ease of processing, polymers have become one of the most desired materials for engineering applications. Consequently, the past few decades have shown a great expansion in the number of research related to polymer nanocomposites due to the development of advanced materials for potential applications. Epoxy, in particular, is a widely used thermoset material in aerospace, automotive, and marine applications due to its superior mechanical properties, thermal stability, solvent resistance, and ease of processing [1,2]. Epoxy is also great as a matrix to produce nanocomposites. Epoxy-based nanocomposites, especially with carbon nanofillers, have numerous potential applications, such as for thermal management, electronics, fuel cells, and transportation [2,3].

Halloysite is a fine clay mineral consisting of tubular particles, with a multi-layered wall structure. In recent years, interest in the application of HNTs in polymer materials has grown. Our previous work has shown that HNTs, as low-cost nanotubes, can significantly improve the mechanical properties of epoxy [4]. Ye et al. reported that the incorporation of 2.3 wt% of HNTs into epoxy has increased the Charpy impact strength up to approximately four times [5]. CNTs, which were discovered by Ijima in 1991, are known as one of the stiffest engineering materials [6]. CNTs are great as nanofillers for aerospace applications due to their unique chemical and physical properties, even at a low fraction [7]. CNTs are widely used as reinforcements for various matrices, such as ceramics, polymers, and metals. Epoxy nanocomposites reinforced with 0.25 wt% of CNTs showed 58% improvement in flexural strength compared to pure resin [7]. Montazeri reported improvements of 15% and 11% in elastic modulus and tensile strength for epoxy reinforced with 1 wt% of CNTs [8].

HNTs were also compared with CNTs in poly(lactic acid) (PLA) and polyurethane. The tensile strength of the PLA matrix was increased by CNTs, but was decreased by HNTs, with increasing filler content [9]. Meanwhile, the elongation at break and the impact strength were decreased with increasing CNTs content, yet these properties were relatively unchanged with increasing HNTs content. When thermoplastic polyurethane (TPU) was used as an impact modifier/compatibilizer, the addition of HNTs has further increased the impact strength and the elongation at break of the matrix, since the short and straight HNTs were pulled out from the extensible toughened matrix [9]. Hybridisation in composites is performed to alter properties to meet certain demands and to neutralise the disadvantages of one component by adding another [10].

Gissinger et al. studied the nanoscale structure and properties of polyacrylonitrile (PAN)/CNTs composites [11]. In their study, the interfacial shear strengths of the composites were improved by adding CNTs with a smaller diameter and with PAN pre-orientation. Based on a molecular dynamics simulation, the lowest interfacial shear strength was discovered in amorphous PAN, added with CNTs with a similar diameter. The PAN with ~75% crystallinity showed hexagonal configuration of nitrile clusters close and far from the CNT boundary, which could affect carbonisation into regular graphitic structures [11]. Choi et al. studied a multi-scale mechanical model for an effective interphase of SWNT and epoxy nanocomposite. It was observed that the nanotube size could

influence axial stiffness along the nanotube alignment direction. Additionally, the transverse axial and shear stiffness components were lesser than the corresponding values of a neat polymer. The existence of an inner soft and slippery polymer layer in the vicinity of nanocarbon surface was discovered via an analysis of deformation energy and its distribution inside the nanocomposite unit cell [12]. Li et al. reported the mechanical enhancement of the interlayer hybrid of CNTs film/carbon fibre/epoxy composite. The results showed that the ultrathin CNTs film had significantly increased the compression strength of the hybrid composite by 34% compared with carbon fibre/epoxy control composite. The increment could be due to the numerous CNTs interconnection nodes, as well as the excellent interfacial bonding between CNTs network and adjacent carbon fibres [13]. The authors also reported that the CNTs interlayers had increased the glass transition temperature and high storage modulus at the rubbery state of the CNTs/carbon fibre/epoxy hybrid laminates [13].

Many researchers reported that the ideal filler reinforcement is 1 wt% or less because it is difficult to disperse fillers at higher weight fractions and the agglomerates could act as stress concentration sites, thereby, deteriorating the mechanical properties [14–17]. A new strategy was developed to improve the mechanical and thermal properties of epoxy by combining HNTs and CNTs since available studies on the effects of HNTs–CNTs at low loading content are limited. Therefore, the main aim of this study was to investigate the synergistic effects of HNTs–CNTs on the mechanical properties of epoxy nanocomposites at low loading content (1 wt%) and a short sonication time (10 min). The synergistic effects of these two different fillers on the mechanical properties of nanocomposites are also discussed.

2. Materials and method

The epoxy and hardener used in this research were the Miracast 1517A and Miracast 1517B supplied by Miracon Sdn. Bhd., Seri Kembangan, Malaysia. The densities of the epoxy and hardener were 1.13 and 1.1 g/cm³, respectively. This type of epoxy system is normally used in the composites industry for its low viscosity. The low viscosity of the hardener helps to improve the dispersion and the fast curing of the nanocomposites to prevent agglomeration. The gelation time of the resin was 40 min at room temperature (RT). The HNTs used in this research were acquired from Sigma Aldrich, UK. The diameter and length of HNTs were 30–70 nm and 1–4 μm, respectively. Similar to montmorillonite, halloysite consists of two layers of aluminosilicate at 1:1 Al to Si ratio. The CNTs that comprised of approximately 5–20 graphitic layers used in this research were purchased from Sigma Aldrich, UK. The CNTs were 7–15 nm in diameter and 0.5–10 μm in length. SEM images of HNTs and CNTs taken by FESEM (Zeiss, Germany) are shown in Figure 1.

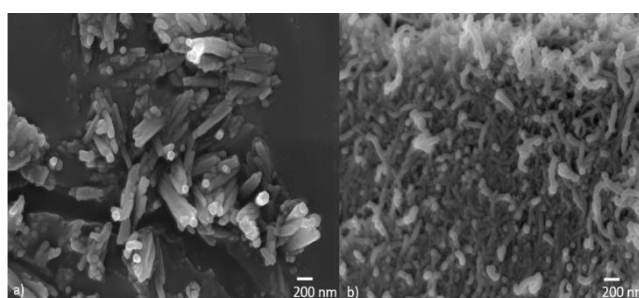


Figure 1. FESEM images: (a) HNTs, and (b) CNTs.

To produce hybrid nanocomposites samples, 0.5 wt% of HNTs and 0.5 wt% of CNTs were dispersed in epoxy resin at room temperature for 10 min using a 100 Watt bath sonicator at 40 kHz, followed by vacuum degassing for 10 min. Then, the hardener was manually mixed with the HNTs/CNTs-filled epoxy. The resin was poured into silicone moulds and cured at room temperature for 12 h, followed by postcuring at 120 °C for 5 h, as recommended by the supplier (Miracon Sdn. Bhd.) to achieve complete crosslinking. Similar procedures were performed for 1 wt% HNTs–epoxy and 1 wt% CNTs–epoxy. To prepare the monolithic epoxy, epoxy resin was sonicated for 10 min, mixed with the hardener, and poured into silicone moulds. The curing process was similar to the curing process for the nanocomposites.

2.1. Characterisation

A Dynamic Mechanical Analyser (DMA 8000, Perkin-Elmer) was used to determine the dynamic storage modulus (E') and loss modulus (E'') of the samples. The loss factor, $\tan \delta$, was calculated as the ratio of E''/E' . Rectangular test specimens were prepared at $35 \times 6 \times 3$ mm dimensions. All tests were conducted using the temperature sweep method (temperature ramp of 40 to 140 °C at 5 °C min^{-1}) at a constant frequency of 1 Hz. Tensile properties were measured according to ASTM D638 Type-V geometry, with specimen thickness of 3 mm. The displacement rate was set at 1 mm/min. A flexural test was performed using the Victor Universal Testing Machine (Victor VE 2302). Five specimens were tested for each composition. The displacement rate for the tensile tests was set at 1 mm/min. The flexural tests were conducted according to ISO 178, with a specimen thickness of 4 mm. The fracture toughness (K_{IC}) was obtained using a single edge notch three-point bending (SEN-TPB) specimen (ASTM D5045). The displacement rate was set at 1 mm/min. The dimensions were $3 \times 6 \times 36$ mm, with a crack length of 3 mm at the centre of the sample. K_{IC} was calculated using the linear fracture mechanics following the relationship shown by the following Eq 1:

$$K_{IC} = \frac{P_{max}(\frac{a}{w})}{BW^{1/2}} \quad (1)$$

where $f(a/w)$ is the calibration factor for the samples, which can be calculated using the following Eq 2:

$$f(\frac{a}{w}) = \frac{[(2 + \frac{a}{w})\{0.0866 + 4.64(\frac{a}{w})^2 + 14.72(\frac{a}{w})^3 - 5.6(\frac{a}{w})^4\}]}{(1 - \frac{a}{w})^{3/2}} \quad (2)$$

The critical strain energy release rate (G_{1C}) was calculated using Eq 3, where E is the Young's modulus obtained from the tensile tests (MPa), and ν is the Poisson's ratio of the polymer, taken to be 0.35.

$$G_{1C} = \frac{K_{1C}^2(1 - \nu^2)}{E} \quad (3)$$

Vickers microhardness test was performed using the Buehler Micromet II for the monolithic epoxy and its nanocomposites. The 200 g load was applied for 10 s and the readings were taken from the samples according to standard ISO 178. Images of the broken samples from the flexural test were analysed using a mini Field Emission Scanning Electron Microscope (FESEM, Zeiss, Germany).

Figure 2 shows the dimensions of all specimens used in this research, which include DMA, tensile, flexural, and three-point-bend samples (mode I fracture toughness).

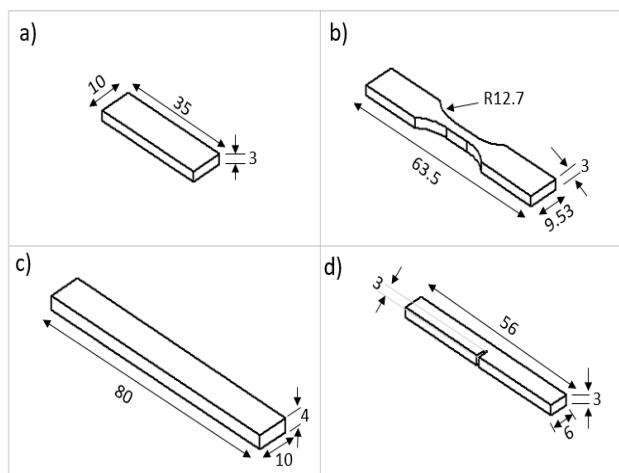


Figure 2. Three dimensional models of test specimens: (a) dynamic mechanical analysis, (b) tensile, (c) flexural, and (d) single-edge-notch for the three-point bend (mode I fracture toughness, K_{IC}). All dimensions are in mm.

3. Results and discussions

Table 1 summarises the values of $\tan \delta$ and T_g of the monolithic epoxy and its nanocomposites. The hybrid nanocomposites (0.5 wt% HNTs–0.5 wt% CNTs) recorded the lowest $\tan \delta$ (0.61) and the highest T_g (116.3 °C) compared to the other samples. The increased T_g can be attributed to the adsorbed layer effect as the polymer chains were being tied down by the surface of the nanotubes [14,18]. The low value of T_g (94.5 °C) with 1 wt% of CNTs can be linked to the aggregation of fillers caused by poor dispersion due to inadequate sonication time. Figure 3 shows the storage moduli for the monolithic epoxy and its nanocomposites. Monolithic epoxy recorded the lowest storage modulus value at 1.344 GPa. With the addition of 1 wt% of CNTs and 1 wt% of HNTs, the storage modulus increased up to 2% and 14%, respectively. The highest storage modulus was observed with the addition of hybrid nanocomposites (0.5 wt% HNTs–0.5 wt% CNTs) at 47%. The significantly increased mechanical properties of the hybrid nanocomposites can be associated to the different nanostructures and characteristics of the HNTs and CNTs. Both fillers have extremely stiff nanotubes and high strength. Excellent compatibility between these fillers and the epoxy matrix could also play a role in the reinforcing effect, as reported by Liu et al. [18]. Thus, the HNTs–CNTs could chemically be interconnected with the matrix after curing. The good interfacial bonding allowed effective load transfer between the matrix and the rigid phase. Consequently, the nanocomposites exhibited higher modulus even at elevated temperatures. The loss moduli of the monolithic epoxy and its nanocomposites are also presented in Figure 3. Compared to the monolithic epoxy, the loss modulus of the hybrid nanocomposites is increased up to 75% (Figure 4), which is the highest value compared to the loss modulus of 1 wt% of HNTs–epoxy and 1 wt% of CNTs–epoxy nanocomposites. It is known that it is extremely difficult to achieve uniform dispersion of CNTs in epoxy matrix [7]. As observed in the storage modulus and loss curves, samples reinforced with 1 wt% of CNTs have

lower values compared with the values for hybrid and 1 wt% HNTs–epoxy samples. Results showed that 1 wt% of HNTs and lesser have better dispersion in epoxy matrix, even with short sonication durations [14,19,20]. HNTs and CNTs are known to restrict the mobility of the polymer chains, thereby, causing an increase in storage moduli and loss moduli [1,21].

Table 1. $\tan \delta$ and T_g of monolithic epoxy and its nanocomposites.

Sample	$\tan \delta$	T_g (°C)
Monolithic Epoxy	0.64	105.1
0.5 wt% HNTs–0.5 wt% CNTs	0.61	116.3
1 wt% of HNT	0.62	113.6
1 wt% of CNTs	0.4	94.5

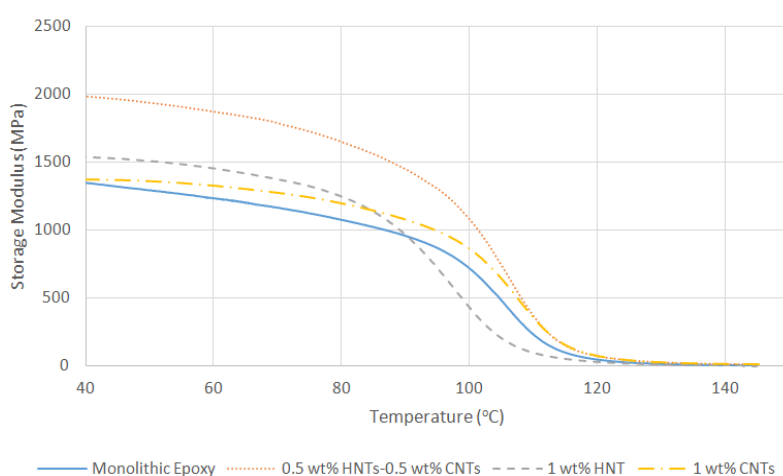


Figure 3. Storage modulus of monolithic epoxy and its nanocomposites.

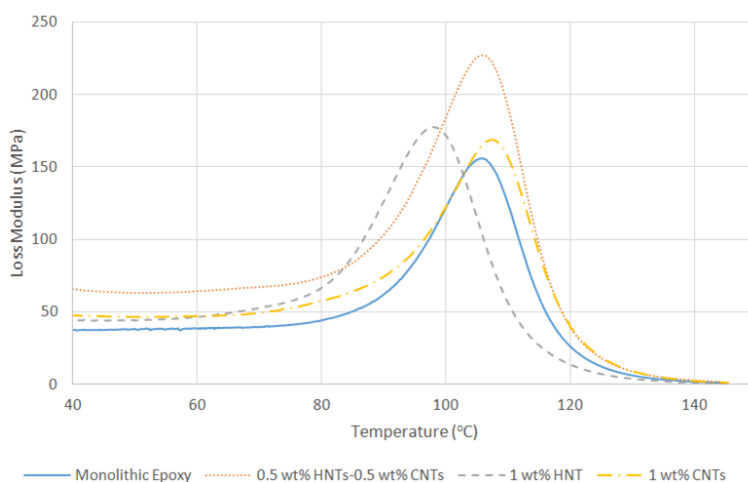


Figure 4. Loss modulus of monolithic epoxy and its nanocomposites.

The variations in the tensile strength of the nanocomposites are shown in Figure 5a. Monolithic epoxy recorded the lowest tensile strength with 33 MPa. The minimum tensile strength improvement

of 4% was observed for the 1 wt% CNTs–epoxy nanocomposites. As for the 1 wt% HNTs–epoxy nanocomposites, the tensile strength was increased up to 33%, while the hybrid nanocomposites recorded a significant improvement of 45%. Figure 5b shows the Young’s modulus for the epoxy nanocomposites, where the highest improvement was observed for the hybrid nanocomposites. This significant improvement clearly suggests the synergistic effects of the hybrid fillers.

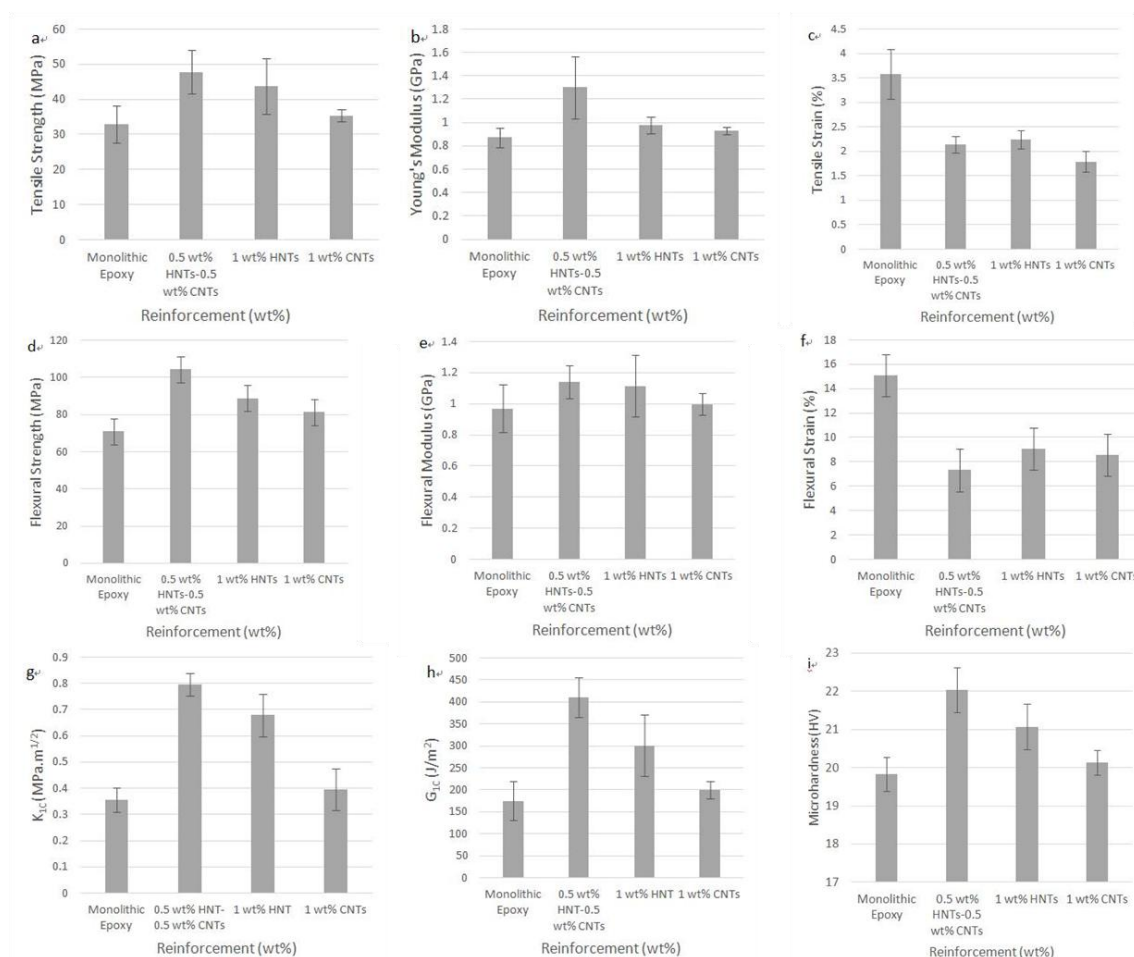


Figure 5. Mechanical properties of epoxy nanocomposites: (a) tensile strength, (b) Young’s modulus, (c) tensile strain, (d) flexural strength, (e) flexural modulus, (f) flexural strain, (g) K_{IC} , (h) G_{IC} , and (i) microhardness.

CNTs can act as extended tentacles that can become entangled with the polymer chains, resulting in stronger interfacial interactions between the matrix and the reinforcement. The tensile strain values are shown in Figure 5c. In general, tensile strain was decreased for samples reinforced with the nanofillers compared with the monolithic epoxy. The tensile strain ranged between 1.8% and 2% for the nanocomposites, whilst the monolithic epoxy recorded tensile strain of 3.6%. The values of flexural strength are shown in Figure 5d. The effect of hybrid nanofillers on flexural properties was very impressive. The flexural strength of the hybrid nanocomposites was increased up to 46%. As for the 1 wt% CNTs–epoxy and the 1 wt% HNTs–epoxy samples, their flexural strength was increased up to 14% and 25%, respectively. Figure 5e shows the flexural moduli of all samples.

Monolithic epoxy recorded the lowest flexural modulus, with 0.97 GPa, followed by the 1 wt% CNTs–epoxy nanocomposites, with 1 GPa (3% increase). The maximum flexural modulus was recorded for hybrid nanocomposites, with 17% of improvement. For samples reinforced with 1 wt% of HNTs, the increase in flexural modulus was only 3.1%.

Figure 5f shows the values of flexural strain for the nanocomposites. The hybrid nanocomposites showed the lowest flexural strain of approximately 7% and the highest was observed at 15% for monolithic epoxy. As for epoxy samples reinforced with 1 wt% of CNTs and 1 wt% of HNTs, their flexural strain was 8.6% and 9%, respectively. At the interface of the HNTs–CNTs and the epoxy matrix, interfacial oxygen atoms and internal stress created chemical bonding and mechanical bonding that improved the load transfer from the matrix to the nanofillers [22]. The values of fracture toughness, K_{IC} , are presented in Figure 5g. The maximum improvement was observed for the hybrid nanocomposites, with an increase of up to 125%. The minimum increase in fracture toughness was observed for the sample with 1 wt% of CNTs–epoxy (12.7%). Figure 5h shows the values of critical strain energy release rate (G_{IC}) for all samples. The maximum G_{IC} was achieved by the hybrid nanocomposites, with 134% increase. As for the 1 wt% CNTs–epoxy and the 1 wt% HNTs–epoxy, their G_{IC} was increased by 14% and 72%, respectively. Figure 5i shows the values of Vickers microhardness for all nanocomposite systems. The maximum increase in microhardness was observed for the hybrid nanocomposites (11%). Samples reinforced with CNTs showed an improvement of 1.5%, while the microhardness of 1 wt% HNTs–epoxy was increased by 6%. Figure 6 shows the optical micrograph of Vickers indentation tests. Similar to the results presented earlier, only small percentages of improvement in microhardness were observed. The smallest indentation was observed for the hybrid nanocomposites.

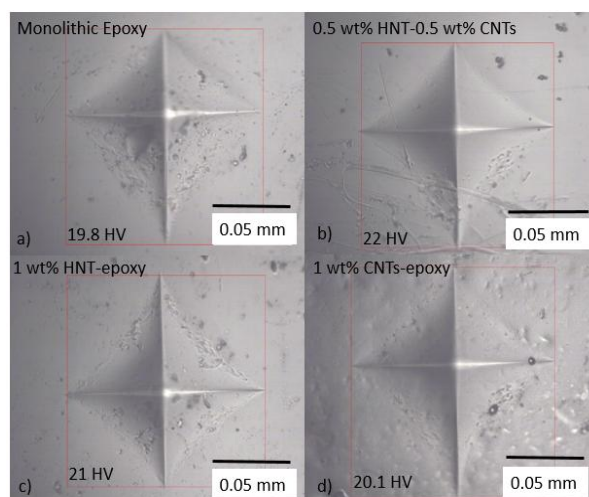


Figure 6. Indentations of Vickers microhardness for monolithic epoxy and its nanocomposites: (a) monolithic epoxy with the average microhardness of 19.8 HV, (b) 0.5 wt% HNTs–0.5 wt% CNTs–epoxy (22 HV), (c) 1 wt% HNTs–epoxy (21 HV), and (d) 1 wt% CNTs–epoxy (20.1 HV).

The failure process of these nanocomposites is analysed using FESEM and the fracture surfaces of the samples are shown in Figure 7. Figure 7a shows the image of monolithic epoxy, whereby the smooth surface and straight crack propagation indicate a brittle fracture. Figure 7b shows the image

of the hybrid nanocomposites, where the cracks emanate radially. The surface of the hybrid nanocomposites appeared to be coarser than that of monolithic epoxy, and beeline crack propagation was not apparent. Hence, the fracture mechanism would have been a semi-ductile. This synergistic effect could be attributed to the excellent contact within the stabilised mixture of HNTs and CNTs against agglomeration, which enabled better dispersion within the polymer matrix. Hence, the contact surface area within the hybrid nanofillers was significantly increased [23]. The SEM image in Figure 7b also shows the HNTs–CNTs crack bridging and crack deflection, which could explain the toughening mechanism. Figure 7c shows the image of the 1 wt% HNTs–epoxy sample, where long, straight and elevated crack lines can be observed. The HNTs could have been positioned in such a way that initiated the cracks to propagate along a specific direction. Figure 7d shows the image of the 1 wt% CNTs–epoxy sample, where localised uneven surface and flat crack lines indicate CNTs agglomeration and poor interfacial interactions.

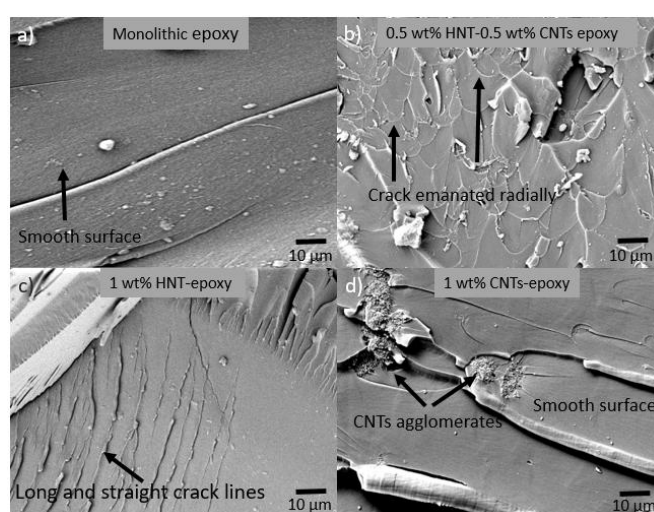


Figure 7. FESEM images of monolithic epoxy and its nanocomposites.

4. Conclusions

The synergistic effects of hybrid nanofillers (HNTs + CNTs) on the mechanical properties of epoxy nanocomposites were investigated. The addition of 0.5 wt% of HNTs and 0.5 wt% of CNTs has significantly improved the mechanical properties of epoxy. The tensile strength and Young's modulus were increased up to 45% and 49%, respectively. The flexural strength was increased up to 46%, whilst the flexural modulus was increased up to 17%. Fracture toughness (K_{IC}) and critical strain energy release rate (G_{IC}) recorded improvements of 125% and 134%, respectively. As shown in the FESEM images of the hybrid nanocomposites, the formation of microcracks that emanated radially and the increased fracture surface area due to crack deflection were the major toughening mechanisms in the hybrid nanocomposites. This study has shown that the synergistic effects of HNTs–CNTs hybrid nanofillers at low content (0.5 wt% HNTs–0.5 wt% CNTs) were sufficient to improve the mechanical properties of epoxy. However, more research should be conducted to study the mechanical properties of hybrid nanocomposites at different loadings and in different environments.

Acknowledgements

The authors would like to thank Universiti Kuala Lumpur Malaysia Italy Design Institute (UniKL MIDI), the Malaysian Nuclear Agency, and Northumbria University, UK for the provision of research facilities, without which the analyses of relevant data would not have been possible. This research was funded by an internal grant (STRG 18052) from the Universiti Kuala Lumpur, Malaysia.

Conflict of interests

The authors declare no conflict of interests.

References

1. Saharudin MS, Hasbi S, Rashidi NM, et al. (2018) Effect of short-term water exposure on mechanical properties of multi-layer graphene and multi-walled carbon nanotubes-reinforced epoxy nanocomposites. *J Eng Sci Technol* 13: 4226–4239.
2. Wei J, Saharudin MS, Vo T, et al. (2017) N,N-Dimethylformamide (DMF) usage in epoxy/graphene nanocomposites: problems associated with reaggregation. *Polymers* 9: 193.
3. Atif R, Wei J, Shyha I, et al. (2016) Use of morphological features of carbonaceous materials for improved mechanical properties of epoxy nanocomposites. *RSC Adv* 6: 1351–1359.
4. Saharudin MS, Wei J, Shyha I, et al. (2016) The degradation of mechanical properties in halloysite nanoclay-polyester nanocomposites exposed in seawater environment. *J Nanomater* 2016: 1–12.
5. Ye Y, Chen H, Wu J, et al. (2011) Interlaminar properties of carbon fiber composites with halloysite nanotube-toughened epoxy matrix. *Compos Sci Technol* 71: 717–723.
6. Peeterbroeck S, Alexandre M, Nagy JB, et al. (2004) Polymer-layered silicate-carbon nanotube nanocomposites: unique nanofiller synergistic effect. *Compos Sci Technol* 64: 2317–2323.
7. Luhyna N, Inam F (2012) Carbon nanotubes for epoxy nanocomposites: a review on recent developments. *2nd International Conference on Advanced Composite Materials and Technologies for Aerospace Applications*, 80–86.
8. Montazeri A, Montazeri N (2011) Viscoelastic and mechanical properties of multi walled carbon nanotube/epoxy composites with different nanotube content. *Mater Des* 32: 2301–2307.
9. Erpek CEY, Ozkoc G, Yilmazer U (2017) Comparison of natural halloysite with synthetic carbon nanotubes in poly(lactic acid) based composites. *Polym Compos* 38: 2337–2346.
10. Inam F, Wong DWY, Kuwata M, et al. (2010) Multiscale hybrid micro-nanocomposites based on carbon nanotubes and carbon fibers. *J Nanomater* 2010: 1–12.
11. Gissinger JR, Pramanik C, Newcomb B, et al. (2017) Nanoscale structure-property relationships of polyacrylonitrile/CNT composites as a function of polymer crystallinity and CNT diameter. *ACS Appl Mater Interfaces* 10: 1017–1027.
12. Choi J, Shin H, Cho M (2016) A multiscale mechanical model for the effective interphase of SWNT/epoxy nanocomposite. *Polymer* 89: 159–171.
13. Li T, Li M, Gu Y, et al. (2018) Mechanical enhancement effect of the interlayer hybrid CNT film/carbon fiber/epoxy composite. *Compos Sci Technol* 166: 176–182.

14. Saharudin MS, Atif R, Shyha I, et al. (2017) The degradation of mechanical properties in halloysite nanoclay-polyester nanocomposites exposed to diluted methanol. *J Compos Mater* 51: 1653–1664.
15. Saharudin MS, Shyha I, Inam F (2016) The effect of methanol exposure on the flexural and tensile properties of halloysite nanoclay/polyester. *Int J Adv Sci Eng Technol* 4: 42–46.
16. Rull N, Ollier RP, Francucci G, et al. (2015) Effect of the addition of nanoclays on the water absorption and mechanical properties of glass fiber/up resin composites. *J Compos Mater* 49: 1629–1637.
17. Ollier R, Rodriguez E, Alvarez V (2013) Unsaturated polyester/bentonite nanocomposites: Influence of clay modification on final performance. *Compos Part A-Appl S* 48: 137–143.
18. Liu M, Guo B, Du M, et al. (2008) Natural inorganic nanotubes reinforced epoxy resin nanocomposites. *J Polym Res* 15: 205–212.
19. Alamri H, Low IM (2012) Effect of water absorption on the mechanical properties of nano-filler reinforced epoxy nanocomposites. *Mater Des* 42: 214–222.
20. Gorrasi G, Pantani R, Murariu M, et al. (2014) PLA/halloysite nanocomposite films: water vapor barrier properties and specific key characteristics. *Macromol Mater Eng* 299: 104–115.
21. Saharudin MS, Atif R, Inam F (2017) Effect of short-term water exposure on the mechanical properties of halloysite nanotube-multi layer graphene reinforced polyester nanocomposites. *Polymers* 9: 27.
22. Chen X, Bao R, Yi J, et al. (2019) Enhancing interfacial bonding and tensile strength in CNT–Cu composites by a synergetic method of spraying pyrolysis and flake powder metallurgy. *Materials* 12: 670.
23. Yang SY, Lin WN, Huang YL, et al. (2011) Synergetic effects of graphene platelets and carbon nanotubes on the mechanical and thermal properties of epoxy composites. *Carbon* 49: 793–803.



AIMS Press

© 2019 the Author(s), licensee AIMS Press. This is an open access article distributed under the terms of the Creative Commons Attribution License (<http://creativecommons.org/licenses/by/4.0>)